AMERICAN SOCIETY FOR MICROBIOLOGY | Applied and Environmental Microbiology®

BIOTECHNOLOGY

Nitrogen Fixation and Ammonium Assimilation Pathway Expression of *Geobacter sulfurreducens* Changes in Response to the Anode Potential in Microbial Electrochemical Cells

Juan F. Ortiz-Medina,[a] Mark R. Poole,[a] Amy M. Grunden,[b] Douglas F. Call[a]

[a]Department of Civil, Construction, and Environmental Engineering, North Carolina State University, Raleigh, North Carolina, USA

[b]Department of Plant and Microbial Biology, North Carolina State University, Raleigh, North Carolina, USA

ABSTRACT Nitrogen gas (N_2) fixation in the anode-respiring bacterium *Geobacter sulfurreducens* occurs through complex, multistep processes. Optimizing ammonium (NH_4^+) production from this bacterium in microbial electrochemical technologies (METs) requires an understanding of how those processes are regulated in response to electrical driving forces. In this study, we quantified gene expression levels (via RNA sequencing) of *G. sulfurreducens* growing on anodes fixed at two different potentials (−0.15 V and +0.15 V versus standard hydrogen electrode). The anode potential had a significant impact on the expression levels of N_2 fixation genes. At −0.15 V, the expression of nitrogenase genes, such as *nifH*, *nifD*, and *nifK*, significantly increased relative to that at +0.15 V, as well as genes associated with NH_4^+ uptake and transformation, such as glutamine and glutamate synthetases. Metabolite analysis confirmed that both of these organic compounds were present in significantly higher intracellular concentrations at −0.15 V. N_2 fixation rates (estimated using the acetylene reduction assay and normalized to total protein) were significantly larger at −0.15 V. Genes expressing flavin-based electron bifurcation complexes, such as electron-transferring flavoproteins (EtfAB) and the NADH-dependent ferredoxin:NADP reductase (NfnAB), were also significantly upregulated at −0.15 V, suggesting that these mechanisms may be involved in N_2 fixation at that potential. Our results show that in energy-constrained situations (i.e., low anode potential), the cells increase per-cell respiration and N_2 fixation rates. We hypothesize that at −0.15 V, they increase N_2 fixation activity to help maintain redox homeostasis, and they leverage electron bifurcation as a strategy to optimize energy generation and use.

IMPORTANCE Biological nitrogen fixation coupled with ammonium recovery provides a sustainable alternative to the carbon-, water-, and energy-intensive Haber-Bosch process. Aerobic biological nitrogen fixation technologies are hindered by oxygen gas inhibition of the nitrogenase enzyme. Electrically driving biological nitrogen fixation in anaerobic microbial electrochemical technologies overcomes this challenge. Using *Geobacter sulfurreducens* as a model exoelectrogenic diazotroph, we show that the anode potential in microbial electrochemical technologies has a significant impact on nitrogen gas fixation rates, ammonium assimilation pathways, and expression of genes associated with nitrogen gas fixation. These findings have important implications for understanding regulatory pathways of nitrogen gas fixation and will help identify target genes and operational strategies to enhance ammonium production in microbial electrochemical technologies.

KEYWORDS electromicrobiology, *Geobacter*, nitrogen fixation

Using microorganisms to convert nitrogen gas (N_2) into ammonium (NH_4^+) through biological nitrogen fixation (BNF) offers a sustainable alternative to the carbon-, water-, and energy-intensive Haber-Bosch process. Almost all of the ammonia (NH_3, the

Editor Jennifer B. Glass, Georgia Institute of Technology

Address correspondence to Douglas F. Call, dfcall@ncsu.edu.
The authors declare no conflict of interest.
Received 7 December 2022
Accepted 7 March 2023
Published 28 March 2023

deprotonated form of NH_4^+) used in commercial products such as fertilizers, pharmaceuticals, explosives, and cleaning products is produced through the Haber-Bosch process (1). Requiring high temperatures (350 to 550°C) and pressures (150 to 300 atm) (2), this process is responsible for 1.5 to 2.5% of global energy use and 1.6% of CO_2 emissions (3–5). Diazotrophs, such as *Azotobacter vinelandii*, fix N_2 gas under atmospheric conditions, circumventing the need for energy-demanding conditions (6). They have received considerable attention for *in situ* NH_4^+ production in soils (7) and as biocatalysts in biotechnologies (8).

Inhibition of the nitrogenase enzyme by O_2 gas, a major limitation of BNF technologies, can be avoided by using anaerobic microbial electrochemical technologies (METs). For most aerobes, higher O_2 concentrations lead to higher biomass production and respiration rates. In aerobic diazotrophs, the opposite occurs. Higher O_2 concentrations decrease biomass production, and O_2 respiration rates plateau or decrease because O_2 inhibits nitrogenase activity (9, 10). In METs, this problem is avoided, because the anode chamber, where the microorganisms respire, is anaerobic (11). Respiration rates can be elevated by increasing the applied voltage (12). For example, in a single-chamber microbial electrolysis cell (MEC), Ortiz-Medina et al. (13) observed almost 3-fold higher N_2 fixation and NH_4^+ production rates of a mixed consortium when the applied voltage was increased from 0.7 V to 1.0 V.

To better understand and develop NH_4^+-generating METs, fundamental insight into how electrochemical variables impact N_2 fixation is needed. For these goals, bacteria from the family *Geobacteraceae* provide ideal models (14). Many members possess N_2 fixation genes and/or have been reported to fix N_2 (15), and some can generate very high electrical current densities in METs (16). They are also naturally abundant in mixed-culture METs operated under N_2 fixation conditions and have demonstrated N_2 fixation capabilities as single cultures in METs (17). Within the *Geobacteraceae*, *Geobacter sulfurreducens* PCA is a well-studied diazotroph with a fully sequenced genome (15, 18). The N_2 fixation pathway in *G. sulfurreducens* is similar to that in other diazotrophs, but it also has unique aspects, including control of N_2 fixation and NH_4^+ assimilation genes by two two-component His-Asp phosphorelay systems instead of one (19).

One of the most important electrochemical parameters that influences metabolic activity in METs is the anode potential. The anode serves as a terminal electron acceptor. Its potential can be controlled by an external voltage applied with a power supply or potentiostat, leading to different respiration rates and electron transfer mechanisms and pathways (20, 21). For example, the CbcL-dependent pathway has been reported to be essential for electron transfer and is the primary mechanism in *Geobacter*-enriched anodes at potentials below −0.10 V versus standard hydrogen electrode (SHE) (22). However, at more positive potentials, the ImcH-dependent pathway is also activated to harvest additional energy provided by the higher potential (23). This flexibility allows the biocatalytic activity of *G. sulfurreducens* to be responsive to the anode potential. Biomass and current generation increase as the anode potential increases from negative toward more positive values due to higher electron transfer rates; however, above ~0 V versus SHE, additional available energy is not harvested into metabolic energy (24, 25). In contrast, more negative potentials result in accumulation of reduced electron carriers, such as NAD(P)H, that may limit electron transfer rates and compromise redox homeostasis (26, 27). As a result, the cells must find other electron-accepting processes to regenerate electron carriers.

Energy harvesting in response to the anode potential is likely tied to N_2 fixation because a large amount of energy (16 to 18 mol ATP/mol NH_4^+) and strongly reduced electron donors such as ferredoxins and/or flavodoxins are required to produce NH_4^+. Jing et al. (17) found that under N_2 fixation conditions, biomass production decreased and per cell respiration rates increased, suggesting that the cells increased energy-harvesting in response to the increased energy demand of N_2 fixation. Regulatory overlap across N_2 fixation genes and energy and electron transfer-associated genes may also occur in *G. sulfurreducens* (e.g., RpoN involvement in the control of N_2 fixation, NH_4^+ assimilation, pilus

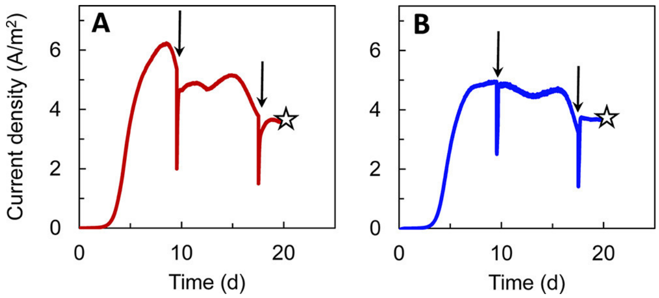

FIG 1 Current density (I_A) profiles of the MECs at (A) a fixed anode potential (E_{AN}) of +0.15 V versus SHE and (B) an E_{AN} of −0.15 V versus SHE, both without NH_4^+ added. Vertical arrows show refeedings. The stars show when RNA was extracted. A single representative curve from triplicates is shown. All replicate curves are available in the supplemental material.

biosynthesis, energy metabolism, and redox homeostasis genes) (28–30). Understanding the genetic and physiological response of *G. sulfurreducens* to nitrogen availability and anode potential is essential for informing genetic and operational strategies that can be leveraged to yield NH_4^+ in METs.

The overarching objective of this study was to determine if N_2 fixation activity and gene regulation change in response to the anode potential. We hypothesized that at more positive anode potentials, N_2 fixation activity would increase because of greater energy availability and current production. To test our hypothesis, we operated MECs with anodes fixed at −0.15 V or +0.15 V. After multiple fed-batch cycles, we extracted and sequenced RNA from the anode biofilms. We also conducted assays to determine N_2 fixation rates and the concentrations of intracellular and extracellular fixed nitrogen products (NH_4^+, glutamine, and glutamate). Our results show that the anode potential has a significant impact on N_2 fixation activity and the regulation of N_2 fixation pathways. Contrary to our hypothesis, we found that N_2 fixation activity increased at −0.15 V, likely due to the cells using the N_2 fixation pathway to maintain redox homeostasis.

RESULTS AND DISCUSSION

Current density profiles of the MECs. After inoculation of the MECs, all reactors displayed similar current density (I_A) trends (Fig. 1). Bacterial colonization of the anode was reflected in a steady increase in I_A (defined as the startup or enrichment phase) due to extracellular electron transfer and consumption of the electron donor (i.e., acetate) until a maximum I_A was reached. Although maximum I_A was slightly higher at +0.15 V, the difference was not found to be significant ($P > 0.05$, t test) due to the higher variability of I_A and startup time (defined as the time at which each reactor achieved an I_A of >0.1 A/m²) during the first batch (Table S1). Replenishment of growth medium led to a slow decrease in I_A compared to the previous cycle. For the second and third cycles, I_A decreased by around 25% and 10% at +0.15 V and −0.15 V, respectively, from the maxima obtained in the previous cycle (Fig. 1A and B). Possible reasons for these decreases include the brief exposure to atmospheric oxygen during medium replacement, as the reactors were moved to an aerobic biological safety cabinet to avoid contamination, and the high acetate concentration (2 g/L or 24 mM) utilized in these experiments. Operating the MECs under an atmosphere of 100% N_2 (to maximize nitrogen availability) instead of the typical gas composition of N_2-CO_2 (80%/20%) (31) may also have impacted bacterial growth and current output, especially if additional CO_2 is needed to support better growth of *G. sulfurreducens*. Utilizing the latter atmosphere and a bicarbonate-based buffer may provide optimal growth conditions in future experiments. Despite cycle-to-cycle variations, when we extracted RNA, the replicates for each treatment exhibited very low variability in I_A, which was important for obtaining reproducible gene expression profiles (Table S1). Given the maturity of the biofilm that occurs after several days of operation, it is likely that some cells within the biofilm were inactive, as anode biofilms can exhibit activity and gene expression stratification depending on the growth stage and thickness (32). Harvesting RNA from *G. sulfurreducens* under exponential-growth conditions (i.e., during biofilm formation at the first cycle) or from sectioned biofilms (33) may help to gain a finer resolution in the gene expression profiles.

When NH_4^+ was present, I_A values were much lower than when N_2 was the sole nitrogen source (Fig. S1). For example, in reactors operating at +0.15 V with either 5 or 10 mM NH_4^+, maximum I_A was 43% lower than that in the treatment at the same anode potential (E_{AN}) without NH_4^+ (Table S1). While this decrease in current may be associated with microbial stress, a concentration of 5 mM NH_4^+ is frequently used in growth media for MEC studies involving *Geobacter* species (12), and the higher concentration was below values (>15 mM NH_4^+) that are reported to cause a significant decrease in current and biomass production in MECs (34). Our results showing that larger current densities occur when no fixed nitrogen is present are consistent with prior studies and suggest that there may be a physiological link between anode respiration and N_2 fixation (35).

Gene expression profiles. (i) Transcriptome data summary. Gene expression profiles of *G. sulfurreducens* under N_2 fixation conditions (no NH_4^+ added) were compared across MECs operating at the two anode potentials. The transcriptome of reactors operating at +0.15 V was the reference. From the approximately 3,430 genes that were identified during analysis, a total of 290 genes were differentially expressed in reactors operated at −0.15 V (Table S2). We defined differential expression as a $\log_2$ fold change ($\log_2$FC) of >2.00 and a *P* value of <0.05 based on previous studies that aimed to minimize false discovery rates (FDR) and biologically nonsignificant genes (36–38). Based on this definition, differentially expressed genes are those that are most responsive to the change in anode potential, while non-differentially expressed genes are, in the majority, constitutively expressed genes and/or are unaffected by anode potential. We grouped differentially expressed genes by metabolic function (e.g., N_2 fixation, electron transfer activity, etc.) based on gene ontology and assigned annotations for *G. sulfurreducens* PCA from the Gene Ontology (GO) and Ensembl databases (39, 40). Additionally, a total of 1,133 genes had a significant difference in expression with respect to the reference treatment ($P < 0.05$), but the change did not reach the $\log_2$-fold threshold, which is shown in the respective volcano plots as expression distributions (Fig. S2). Many of those genes displayed high normalized gene counts (expressed in reads per kilobase per million mapped reads [RPKM]) and a $\log_2$FC of >1.00, which implies that they possessed high levels of expression under a specific treatment despite the original threshold not being reached. We included those genes in the discussion below to better describe the impact of our treatments on N_2 fixation. A list of all identified genes with a $|\log_2\text{FC}|$ of >1.00 and a *P* value of <0.05 is provided in Table S3.

(ii) N_2 fixation and NH_4^+ assimilation. The expression of several genes related to N_2 fixation increased when the MECs were operated at −0.15 V with no added NH_4^+ (Fig. 2). Although only two genes that are critical to N_2 fixation (*nifEN* and *nifV*; involved in nitrogenase assembly) were upregulated by more than 2 $\log_2$-fold (2.11 and 2.07, respectively), other genes showed a high number of counts at the negative potential and a $\log_2$FC of >1.00, including genes encoding the nitrogenase enzyme (*nifD*, *nifH*, and *nifK*, $\log_2$FC = 1.53, 1.98, and 1.93) in model *Geobacter* species (15, 18). Genes such as *gnfK* and *gnfR*, which help regulate and express genes for N_2 fixation when fixed nitrogen is low (19), were upregulated at −0.15 V ($\log_2$FC = 3.38 and 3.05), suggesting that N_2 fixation activity increased at that potential. Although it was moderately expressed, gene counts of *amtB* were also higher at −0.15 V ($\log_2$FC = 1.02). This gene encodes an NH_4^+ transporter that is expressed when low concentrations of NH_4^+ are present to help the cell scavenge it from the environment (41). Gene counts for the molybdenum (Mo) transport system genes at −0.15 V were also higher (Fig. S3). *Geobacter* spp. increase expression of this system under N_2 fixing conditions to acquire Mo from the environment (42) because it is an essential component of the Mo-dependent nitrogenase (19). Other regulatory genes involved in N_2 fixation did not display a significant difference ($P > 0.05$) with respect to E_{AN}, such as *draG* and *draT* ($\log_2$FC = −0.77 and 0.97), which are

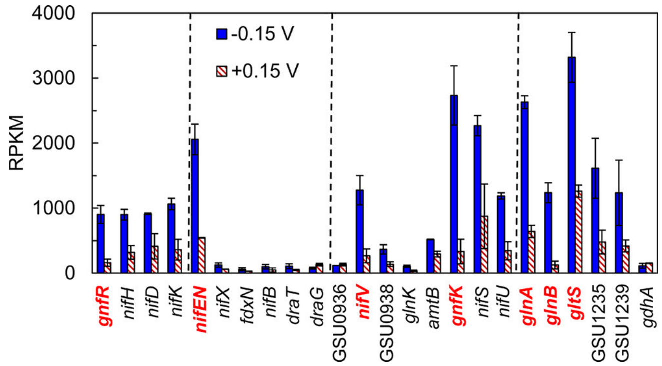

FIG 2 Normalized gene counts of N_2 fixation-associated genes in the MECs operating at E_{AN} of -0.15 V compared to an E_{AN} of $+0.15$ V as a reference. No NH_4^+ was added for both conditions. Red font shows genes that were considered upregulated at an E_{AN} of -0.15 V (i.e., $\log_2FC > 2.00$ and $P < 0.05$). Adjacent genes are grouped based on their location within the genome of *G. sulfurreducens* and are separated by dashed lines. Genes from *glnA* to *gdhA* are included because they are involved in NH_4^+ assimilation after N_2 fixation. Gene counts are expressed in reads per kilobase per million (RPKM). Error bars show the standard deviations for triplicates.

responsible for biochemically modulating nitrogenase reductase activity at a posttranslational level in response to high fixed nitrogen concentrations in other diazotrophs (43, 44). It is known that in other nitrogen-fixing bacteria, *draT* and *draG* expression are constitutive (45), which is consistent with our observed results. Though these regulatory genes are adjacent in the genome of *G. sulfurreducens* to other N_2 fixation genes which were differentially expressed (such as *nifEN*), there is little information on their function and importance in regulating N_2 fixation in this organism.

The NH_4^+ assimilation-relevant genes *glnA*, *glnB*, and *gltS* had high count numbers and were upregulated ($\log_2FC = 2.33$, 3.28, and 2.38, respectively) at -0.15 V (Fig. 2). The gene *glnA*, which encodes glutamine synthetase, enables the reaction of NH_4^+ (either generated through N_2 fixation or present in the medium) with the amino acid glutamate (one amino group) to form glutamine (two amino groups). The gene *glnB*, present in the same operon as *glnA*, is a PII nitrogen-regulatory protein that is expressed under N_2-fixing conditions (19). The gene *gltS* encodes an electron carrier-dependent glutamate synthase that utilizes glutamine as a substrate to regenerate glutamate (via removal of an amino group), effectively acting as an NH_4^+ assimilation and transport mechanism as well as an additional nitrogen-sensing system (46, 47). GSU1235 and GSU1239, which also showed high count numbers but moderate change ($\log_2FC = 1.55$ and 1.23), are also annotated as glutamate synthases (48). Glutamate is sometimes produced by bacteria when osmotic regulation is required in response to a change in solute concentration in the cell's environment (49), as well as when pH decreases (50). If nitrogenase activity is greater at -0.15 V, then higher intracellular NH_4^+ concentrations may develop (50). A counterion such as glutamate may be needed to balance intracellular charge and provide a reactant to convert NH_4^+ to glutamine to avoid osmotic stress (51). Additionally, the production of glutamate and glutamine have been linked to oxidation of electron carriers in other microorganisms, such as *Rhodospirillum rubrum*, when a terminal electron acceptor is limiting (52).

To better understand the relationship between electrode potential and nitrogen fixation, the acetylene reduction assay (ARA) was performed. MECs were assayed after the current stabilized and reached a steady state (~4.5 A/m^2 at -0.15 V and ~6 A/m^2 at $+0.15$ V). MECs at both potentials produced ethylene, confirming that the nitrogenase enzyme in *G. sulfurreducens* was active (Fig. 3A). We normalized the total ethylene production to total anode protein to better compare the two potentials. Fixation at -0.15 V was 246% higher [160 ± 40.5 nmol C_2H_4/(min-mg protein)] compared to $+0.15$ V [65 ± 14.5 nmol C_2H_4/(min-mg protein)] ($P < 0.05$, *t* test). This higher normalized fixation rate is consistent with the upregulation of N_2 fixation-associated genes at -0.15 V discussed above. Although the experiments were performed on mature

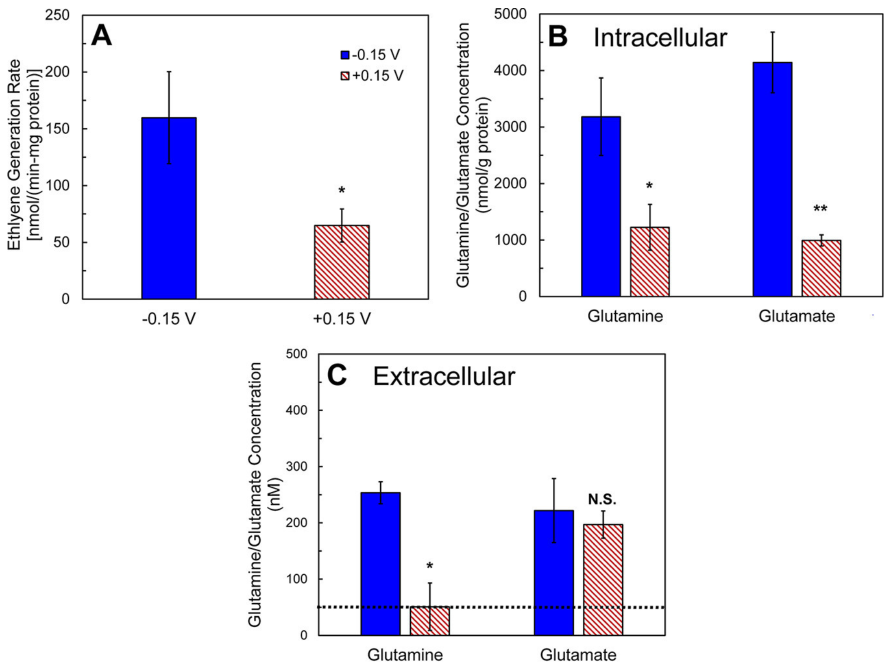

FIG 3 (A) Ethylene generation rates normalized to total biofilm protein in the MECs with anodes fixed at −0.15 V and +0.15 V. Normalized (B) intracellular and (C) extracellular glutamate and glutamine concentrations. The dotted line represents the detection limit of the method. Error bars show the standard deviations for three biological replicates. Asterisks represent the statistical difference (*t* test) between treatments (*, $P < 0.05$; **, $P < 0.01$; N.S., not significant [$P > 0.05$]).

biofilms that may be stratified in activity, our results indicate that the biofilms as a whole had greater N_2 fixation activity at −0.15 V. It is known that other diazotrophs, such as *R. rubrum* and *Rhodopseudomonas palustris*, regenerate electron carriers [e.g., NAD(P)H] under terminal electron acceptor limitations using energy-demanding pathways, among them N_2 fixation, to produce biomass and hydrogen (H_2) (53, 54). It is likely that the observed N_2 fixation activity at −0.15 V is required to maintain redox homeostasis, given that higher NAD(P)H concentrations have been found in *G. sulfurreducens* growing at negative potentials (26). Additionally, it has been reported that at anode potentials above 0 V, such as +0.15 V, lower biomass yields per electron transferred are obtained, likely due to faster removal of electrons from the quinone pool and/or inefficient transfer of electrons to the electrode (25, 55), supporting the notion that −0.15 V offers more efficient conditions for electron transfer and N_2 fixation. The normalized current to biomass and anode surface area from our reactors show higher values at −0.15 V [3.51 ± 0.28 A/(m^2·mg protein)] compared to +0.15 V [2.63 ± 0.17 A/(m^2·mg protein)] ($P < 0.05$, *t* test) which is consistent with this hypothesis. Activity measurements at exponential conditions (i.e., during biofilm formation) should be performed to confirm our findings.

The rates of ethylene generation by *G. sulfurreducens* compare favorably to those of diazotrophs in the literature. Previously, we found that mixed-community MECs produced a maximum of 39 ± 3.7 nmol C_2H_4/(min-mg protein) (13). The results presented here represent an increase of 410% and 167% for −0.15 V and +0.15 V, respectively. A recent study by Jing et al. on N_2 fixation in *G. sulfurreducens* MECs reported rates of 13 nmol C_2H_4/(min-mg protein) for anodes poised at +0.3 V versus saturated calomel electrode (∼+0.54 V versus SHE) (17). Similarly, the free-living diazotroph *A. vinelandii*, considered a model for nitrogenase activity, has been shown to produce between 100 and 250 nmol C_2H_2/(min-mg protein) based on growth conditions (56). Despite lower growth rates, *G. sulfurreducens* generated ethylene comparably to *A. vinelandii* at −0.15 V and at only slightly lower rates at +0.15 V. However, it should be noted that differences in the ARA methodology and normalization (e.g., headspace composition,

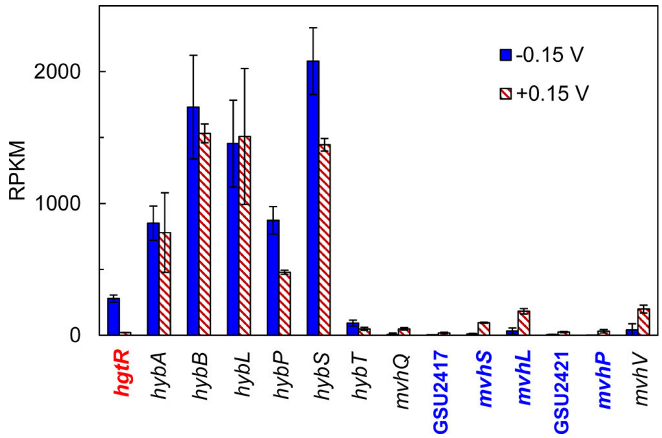

FIG 4 Normalized gene counts of selected genes associated with hydrogenase activity in *G. sulfurreducens* at an E_{AN} of −0.15 V compared to +0.15 V. No NH_4^+ was added in both conditions. Genes shown in bold are classified as differentially expressed ($|\log_2FC| > 2.00$ and $P < 0.05$; red shows upregulated genes; blue shows downregulated genes). Gene counts are expressed in RPKM.

ethylene concentration, and sampling frequency) may contribute to variations across some of these studies.

Since many genes related to NH_4^+ assimilation were upregulated during anode respiration, we measured glutamate and glutamine concentrations in the biomass (intracellular) and medium (extracellular). Intracellular glutamine concentrations were 1,193 ± 118 nM and 809 ± 140 nM at −0.15 V and +0.15 V ($P < 0.05$, *t* test). Glutamate concentrations were 1,564 ± 84 nM and 676 ± 102 nM at −0.15V and +0.15V ($P < 0.01$, *t* test). When normalized to biomass, glutamine and glutamate levels were 260% and 417% higher, respectively, at −0.15 V than at +0.15 V (Fig. 3B). Elevated levels of glutamine at −0.15 V are noteworthy because excess glutamine typically results in downregulation of N_2-fixing genes (57). The fact that elevated glutamine occurred at −0.15 V, which was associated with higher N_2 fixation rates, implies that glutamine may not be a strong repressor of N_2 fixation in *G. sulfurreducens*. This hypothesis is supported by the work of Ueki and Lovley (19), who suggested that N_2 fixation is under the control of a novel two-component system that responds mainly to NH_4^+ limitation. Extracellular glutamine and glutamate were expected to be low because *G. sulfurreducens* lacks a known glutamate or glutamine transporter (58). Extracellular glutamine concentrations were 254 ± 20 nM and 51 ± 42 nM at −0.15 V and +0.15V, respectively ($P < 0.01$, *t* test). Glutamate concentrations, however, were 223 ± 57 nM and 197 ± 24 nM at −0.15 V and +0.15 V, respectively ($P > 0.05$, *t* test) (Fig. 3C). Since the detection limit of the method was 50 nM, the glutamine results at +0.15 V may not be accurate. The low levels of extracellular glutamate and glutamine that were detected are likely due to either general amino acid transporters that act as glutamate/glutamine exporters or cell component breakdown in the medium (59).

(iii) H_2-dependent genes. H_2 gas is an important regulator of some genes and can also serve as an electron donor. In the MECs, H_2 gas is generated by the nitrogenase during N_2 fixation and abiotically at the cathode (60). With respect to growth, genes with high expression counts at −0.15 V included the H_2-dependent growth transcriptional repressor gene *hgtR* (upregulated at −0.15 V; $\log_2FC = 4.19$) (Fig. 4). HgtR represses genes involved in biosynthesis and energy generation when *Geobacter* species use H_2 as an electron donor (29). It is unlikely that cathodically-generated H_2 was responsible for the differential expression of *hgtR*, because the current (which is proportional to H_2 gas generation) at the two potentials was very similar ($P > 0.05$, *t* test) at the time RNA was extracted (Table S1). Since nitrogenase-related genes had higher expression levels at −0.15 V (implying that N_2 fixation was greater at that potential), it is likely that H_2 produced by the nitrogenase was the main driver. Expression of *hgtR* may have diverted electrons from central carbon metabolism and biosynthesis toward N_2 fixation at that

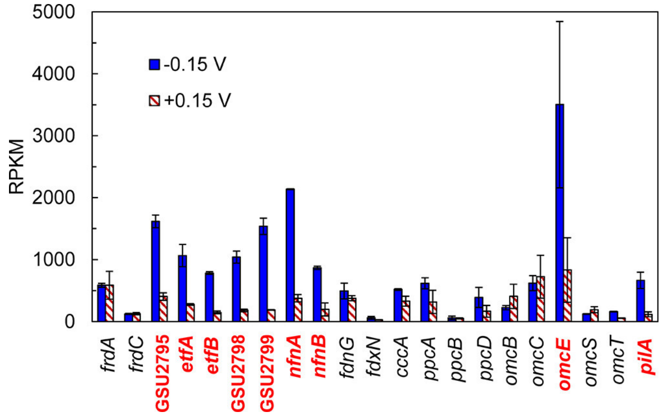

FIG 5 Normalized gene counts of selected genes associated with electron transfer activity in *G. sulfurreducens* at an E_{AN} of −0.15 V versus SHE compared to an E_{AN} of +0.15 V. No NH_4^+ was added in both conditions. Genes shown in red are classified as differentially expressed ($|\log_2FC| > 2.00$ and $P < 0.05$) with respect to +0.15 V. Gene counts are expressed in RPKM.

potential. The fact that both HgtR and N_2 fixation gene expression are mediated by RpoN (28, 29) lends support to a relationship between these processes.

Regarding oxidation of H_2, the majority of hydrogenase genes were not differentially expressed. The *hyb* cluster comprises genes that synthesize a periplasm-oriented, nickel-dependent hydrogenase Hyb, which is used by *G. sulfurreducens* to oxidize H_2 and is frequently upregulated when energy (through ATP production) is required (61, 62). Some of the genes in this cluster, such as *hybS* and *hybP*, showed a slightly higher expression ($\log_2FC = 0.50$ and 0.84) at −0.15 V, which might be related to higher nitrogenase activity that presumably results in a greater ATP requirement; however, the majority of the genes on this cluster were not differentially expressed. Interestingly, the *mvh* cluster, which encodes a cytoplasmic hydrogenase related to the hydrogenases found in methanogens (62), was downregulated at −0.15 V (Fig. 4). These hydrogenases are reported to generate reduced equivalents such as ferredoxins to drive methanogenesis (63). Although expression of these genes was lower than that of the *hyb* cluster, this hydrogenase is also involved in H_2 uptake. The *mvh*-encoded hydrogenase may also be involved in other functions, such as converting forms of reducing power from H_2; however, the specific role and regulation of Mvh remain unclear (62). Regarding the remaining hydrogenases, the gene clusters *hox*, which may be involved in H_2 production (62, 64), and *hya*, likely involved in oxidative stress defense rather than H_2 uptake (65), did not display high counts or differential expression between treatments (data not shown), most likely due to the experimental conditions analyzed (i.e., biofilm anode instead of biofilm cathode and anaerobic conditions when comparing anode potentials). Additional experiments where cathodically-produced H_2 does not influence gene expression may offer a deeper insight into the relationship between the aforementioned H_2 uptake systems and H_2 production due to nitrogenase activity.

(iv) Electron transfer genes. We also examined the expression of genes related to electron transfer in *G. sulfurreducens*. Those genes shared a major portion of the overall expression profile, where 14 genes were upregulated and 11 downregulated at −0.15 V (Fig. S4). This change in expression was expected, because electron transfer kinetics and activity depend on anode potential in METs, and exoelectrogenic bacteria can adapt electron transfer pathways to changes in anode potential (27). When normalized counts were calculated for genes that are known to possess electron transfer activity, we found that the expression of several genes was significantly higher at −0.15 V, including genes that encode flavoproteins, periplasmic proteins, ferredoxins, such as a nitrogen-associated ferredoxin (*fdxN*), and some outer membrane cytochromes (OMCs) (Fig. 5).

Genes encoding the flavin-based electron bifurcating enzyme complexes NfnAB (*nfnA* and *nfnB*) and EtfAB (*etfA*, *etfB*, and the genes GSU2795, GSU2798, and GSU2799, which may be related) were differentially expressed and upregulated at −0.15 V ($log_2FC > 2.50$ for both NfnAB genes, and $log_2FC > 2.00$ for all EtfAB genes) (Fig. 5). Flavin-based electron bifurcation (FBEB) is a recently discovered mechanism of electron transfer in which microorganisms (mainly anaerobic *Bacteria* and *Archaea*) are able to simultaneously transfer electrons from an electron donor to one acceptor at a more positive potential than the donor (exergonic) and another acceptor at a more negative potential than the donor (endergonic) (66, 67). FBEB produces low-potential electron donors like ferredoxins that can drive reactions such as H_2 evolution and whose generation would normally require considerable expenditure of metabolic energy (i.e., ATP) (66, 67). NfnAB, a NADH-dependent reduced ferredoxin:NADPH oxidoreductase, catalyzes the reversible endergonic reduction of $NADP^+$ with NADH by coupling it to the exergonic reduction of $NADP^+$ with reduced ferredoxin, allowing the generation of either NADPH, NADH, or reduced ferredoxin as metabolically needed and thus maintaining the redox balance of these compounds with minimal energy expenditure (68). The electron transfer flavoprotein EtfAB is known to couple the oxidation of NADH with the reduction of ferredoxins (endergonic) by using energy released during the simultaneous reduction of organic compounds such as crotonyl coenzyme A (crotonyl-CoA) (exergonic) (67, 69). Enzyme complexes similar to EtfAB have been identified in diazotrophs. One example is the Fix system, present in the diazotroph *A. vinelandii*, in which NADH oxidation is coupled to the reduction of quinones and either ferredoxins or flavodoxins to obtain electron donors for N_2 fixation (66, 70). In the case of *G. sulfurreducens*, FBEB remains largely unstudied, with only a few studies discussing a possible association with processes such as carboxydotrophic growth, electron transfer, and N_2 fixation (17, 71, 72). Jing et al. (17) found EtfAB and NfnAB to be upregulated in MECs operated under N_2-fixing conditions compared to when NH_4^+ was added, suggesting that these complexes might be involved in the generation of reduced ferredoxins that drive N_2 fixation. Their findings are based on reactors operated at ~+0.54 V versus SHE. Our results suggest that a lower anode potential further encourages electron bifurcation, possibly due to accumulation of NAD(P)H, which in turn drives higher N_2 fixation rates.

The expression of OMCs was also analyzed, as they are usually required by *Geobacter* species to transfer electrons to insoluble electron acceptors, such as iron, manganese, uranium, or anodes in METs (73–75). Among them, *omcE* was highly expressed at −0.15 V ($log_2FC = 2.04$) (Fig. 5). This cytochrome is required for iron(III) oxide reduction (76) and has also been shown to be involved in anode respiration (77, 78). Although its structure was recently elucidated (79), its properties and exact function during electron transfer are still not fully characterized (80). The genes of other well-characterized OMCs that are commonly expressed during anode respiration, such as *omcB* and *omcS* (73, 77), were not differentially expressed ($log_2FC = -1.05$ and −0.68). Although different OMCs have been reported to be expressed depending on anode potential, a more positive potential typically favors the expression of a higher variety of OMCs (81). It is surprising that in our MECs, only *omcE* showed high expression levels and was upregulated at −0.15 V, suggesting that this OMC may have a connection with higher N_2 fixation rates. As unique sets of OMCs are expressed in bacteria with extracellular electron transfer pathways under other redox-related environmental conditions, such as unusual electron acceptors (e.g., uranium and palladium) (42, 82) and limited soluble electron donors (83), this hypothesis is plausible, although further characterization of *omcE* and its regulation under N_2-fixing conditions is required to fully understand this relationship. Other genes associated with electron transfer in *G. sulfurreducens* that are responsive to anode potential, such as *cbcL* and *imcH* (22, 23, 81), were not differentially expressed in our experiments ($log_2FC = -1.09$ and 0.15). Both genes have been reported to be constitutively expressed and their activity regulated at the protein level (23). Here, *cbcL* expression was lower at −0.15 V, which agrees with a study by Ishii et al. (81). Even though *pilA* is not classified within the "electron transfer activity" category, it encodes a critical component for electron transfer to anodes in *G. sulfurreducens* (84). The expression of *pilA* at −0.15 V was

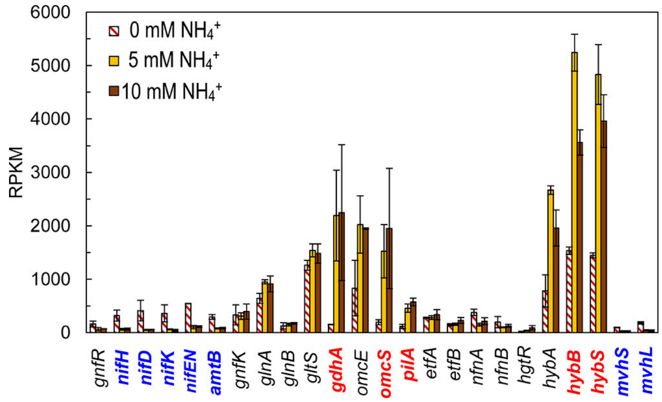

FIG 6 Normalized gene counts of selected genes involved in N_2 fixation, electron transfer activity, and hydrogenase activity in MECs with 5 and 10 mM NH_4^+ compared to 0 mM NH_4^+. All MECs were operated at an E_{AN} of +0.15 V versus SHE. Genes shown in bold are classified as differentially expressed ($|\log_2FC| > 2.00$ and $P < 0.05$; red shows upregulated genes; blue shows downregulated genes). Gene counts are expressed in RPKM.

upregulated ($\log_2FC = 2.48$), which may contribute to higher electron transfer activity. Our protein-normalized current densities support this hypothesis. Current production was higher at −0.15 V [3.51 ± 0.28 A/(m^2·mg protein)] than +0.15 V [2.63 ± 0.17 A/(m^2·mg protein)] ($P < 0.05$, *t* test), despite similar absolute I_A values between E_{AN} values at the time RNA was extracted (Table S1).

(v) Effect of NH_4^+ on gene expression profiles. Gene expression analysis was performed on MECs that operated with either 5 mM or 10 mM NH_4^+ and at +0.15 V to evaluate the impact of NH_4^+ on N_2 fixation. Compared to the reference treatment (no NH_4^+ added, +0.15 V), a total of 193 and 304 genes at 5 mM and 10 mM NH_4^+, respectively, were found to be differentially expressed (Table S4). Lists of all differentially expressed genes are provided in Tables S5 and S6. The addition of NH_4^+ resulted in differential expression of genes related to biosynthesis and reduction in the expression of N_2 fixation genes. Classes of upregulated biosynthesis-related genes included those categorized for translation (e.g., ribosomal proteins) and for protein folding and stabilization (e.g., chaperones), as well as genes encoding NADH dehydrogenases (Fig. S5). These results were expected because sufficient NH_4^+ availability usually suppresses N_2 fixation and makes available the electrons and ATP that would have been used for the metabolically demanding N_2 fixation process (85). The upregulation of genes associated with the tricarboxylic acid (TCA) cycle and genes involved in amino acid production when NH_4^+ was present (Fig. S5) support this hypothesis. These results are also consistent with those obtained by Jing et al. (17), where adding NH_4^+ resulted in upregulation of acetate conversion to biomass, although TCA cycle-related genes were upregulated during N_2 fixation instead. At the physiological level, the higher maximum I_A (which is a direct measure of respiration) when no NH_4^+ was present in the medium (Table S1 and Fig. S1) also supports this hypothesis, as additional electrons from the substrate were likely directed toward N_2 reduction and ATP that otherwise would be used for biomass generation.

The addition of NH_4^+ (at both concentrations) was associated with downregulation of the majority of genes corresponding to N_2 fixation (Fig. 6), which is consistent with prior reports of free-living diazotrophs suppressing N_2 fixation when sufficient NH_4^+ is available. The gene encoding the NH_4^+ transporter *amtB* was also downregulated ($\log_2FC = -2.09$), which was expected, as NH_4^+ at sufficiently high concentrations (more than 1 mM) can diffuse through the membrane in the form of NH_3 (41). Regarding NH_4^+ assimilation genes, *gdhA* was upregulated and highly expressed ($\log_2FC = 3.90$), which supports our findings, as this gene encodes glutamate dehydrogenase, the enzyme responsible for NH_4^+ uptake when sufficient amounts are present, and is known to be repressed under N_2-fixing conditions (19). Accordingly, genes such as *glnA*, *glnB*, and *gltS* were not differentially expressed with NH_4^+ ($\log_2FC$ = 0.53, 0.49, and 0.25), and their expression levels were similar to those obtained with the reference treatment, which is expected, as glutamine synthetase and glutamate synthase are needed to synthesize the respective amino acids during anabolism (86). Many of the electron transfer activity genes known to be highly expressed during anode respiration, such as *omcS*, *omcE*, and *pilA*, showed higher counts with NH_4^+ addition ($\log_2FC$ = 3.03, 1.32, and 2.00) (Fig. 6), most likely in response to the reduced energy expenditure resulting from decreased N_2 fixation or NH_4^+ transporter synthesis (27). Genes found to be associated with electron bifurcation such as *etfA* and *etfB*, were similarly expressed irrespective of NH_4^+ concentration ($\log_2FC$ = 0.10 and 0.14), and *nfnA* and *nfnB* showed only a slight decrease in expression upon NH_4^+ addition ($\log_2FC$ = −1.32 and −1.01) (Fig. 6), suggesting that the positive anode potential (+0.15 V) provided enough energy to facilitate metabolic processes through oxidative phosphorylation. Jing et al. (17) found significant downregulation of all these genes when NH_4^+ was in the medium, which is in general agreement with our observations regarding *nfnA* and *nfnB*. It is likely that the reactor design and operation conditions may explain the differences observed, as their reactors were two-chambered MECs operating at +0.54 V versus SHE and had a maximum I_A of 1.7 A/m^2 (17). Therefore, cathodically-produced H_2 was not available as an electron donor. Possible accumulation of protons may have occurred in their study due to the use of a proton exchange membrane, as commonly reported in these systems (87). These conditions may have further encouraged electron bifurcation to optimize electron transfer toward N_2 fixation and current in comparison to our one-chambered systems, where cathodic H_2 can be reutilized. Regarding hydrogenase-related genes, NH_4^+ addition resulted in upregulation of genes such as *hybB* and *hybS* ($\log_2FC$ = 2.11 and 2.08) (Fig. 6). Based on our current density observations and the repression of nitrogenase activity, the addition of NH_4^+ should result in lower H_2 availability to the anode biofilms. Although counterintuitive, the *hyb* cluster may have been expressed to maximize H_2 uptake and recycle electrons toward biomass production when high concentrations of nutrients (i.e., NH_4^+) are available, which is understandable given that *Geobacter* spp. frequently encounter oligotrophic conditions (88). Since *mvh* genes were also downregulated in the presence of NH_4^+, *G. sulfurreducens* should be able to express different mechanisms of H_2 uptake (and possibly H_2 production) depending on the environmental conditions, as occurs in other microorganisms with several hydrogenase systems (89), although the exact regulation and H_2 affinity of these systems require further study.

(vi) Conceptual models linking N_2 fixation and extracellular electron transfer. Based on the transcriptome profiles described above, we conceived three hypothetical scenarios of N_2 fixation pathways and their regulation in *G. sulfurreducens* as a function of anode potential and availability of NH_4^+. In the first scenario, when the anode potential is +0.15 V and NH_4^+ is available (Fig. 7A), NH_4^+ is readily converted by glutamate dehydrogenase (Gdh) into amino acids, bypassing energy expenditures associated with fixing N_2. Electrons that would have been used for N_2 fixation can instead be directed toward biomass production pathways when NH_4^+ is present. This observation is supported by the lower respiration rates (current densities) recorded when NH_4^+ was present and by the recent study by Jing et al. (17), which showed that electrons are shifted away from biomass production during N_2-fixing conditions while acetate consumption and current production per cell increase.

In the second scenario, the anode potential is +0.15 V and NH_4^+ is absent (Fig. 7B). N_2 fixation and NH_4^+ assimilation pathways through glutamine synthetase (GlnA) and glutamate synthase (GltS) become active. At this positive anode potential, the cells harvest sufficient energy to provide the required electron donors (i.e., ferredoxins/flavodoxins) and ATP for N_2 fixation. Generation of reduced ferredoxins/flavodoxins for N_2 fixation in *G. sulfurreducens* has not been well studied, but common strategies in other diazotrophs include the pyruvate-flavodoxin oxidoreductase (PFOR) present in microorganisms that thrive in anoxic environments (e.g., clostridia and methanogens) (90) and the *Rhodobacter* nitrogen fixation (Rnf) complex utilized by the model diazotroph

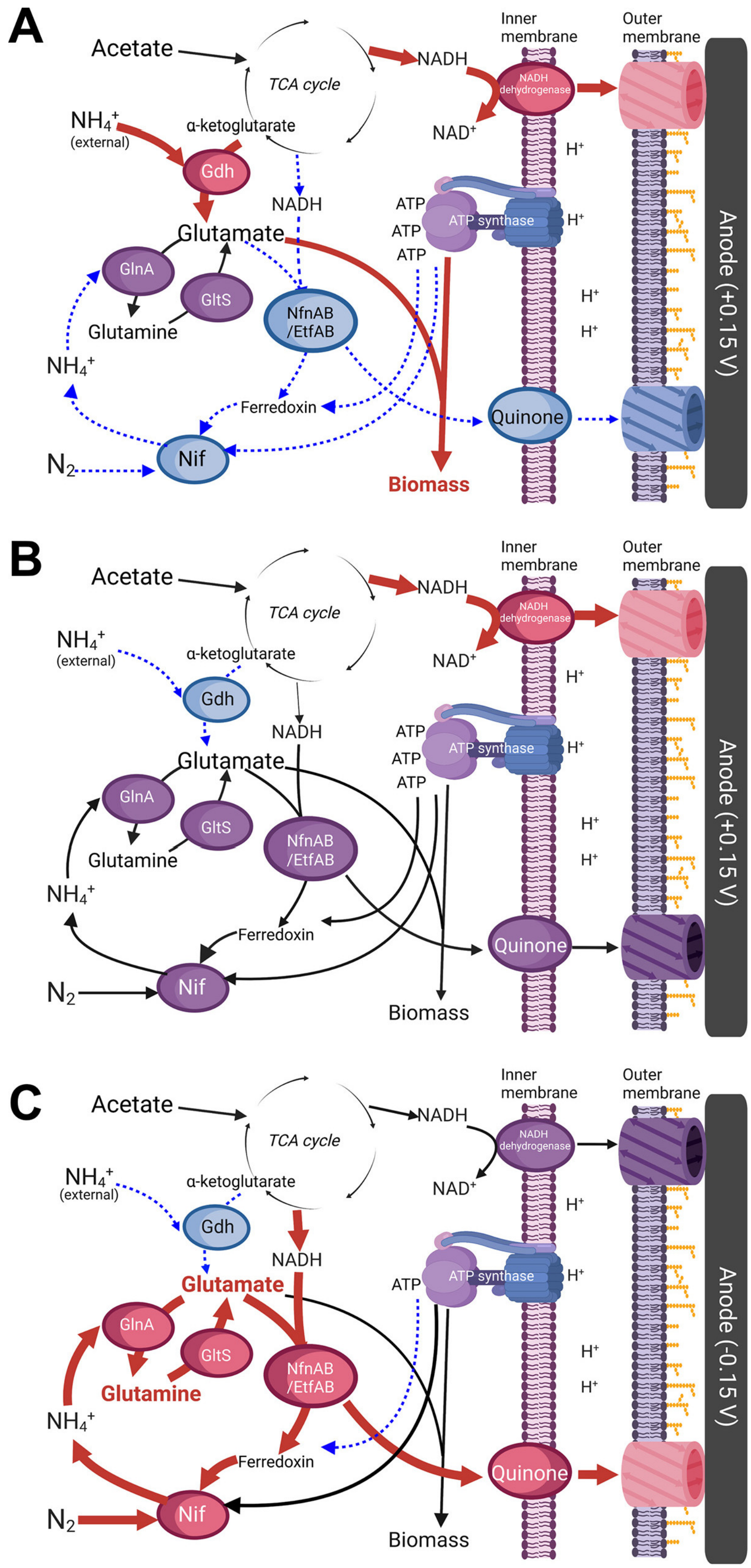

FIG 7 Proposed distribution of electron transfer and metabolic flow in anode-respiring *G. sulfurreducens* (A) at an E_{AN} of +0.15 V and sufficient NH_4^+, (B) at an E_{AN} of +0.15 V and limited NH_4^+, and (C) at an E_{AN} of −0.15 V and limited NH_4^+. Ovals correspond to relevant enzymes present along the flow of electrons/metabolites. Blue ovals and blue dashed lines denote downregulated pathways. Purple ovals and black lines indicate moderate expression and flow under baseline conditions. Red ovals and red bold lines represent upregulated/preferential pathways. Images were created with BioRender.com.

A. vinelandii, which employs translocated protons that otherwise would be destined for further ATP generation (91). Elucidating which strategy (or strategies) is employed by *G. sulfurreducens* to reduce ferredoxins/flavodoxins at positive potentials is important because of the role these electron carriers play in N_2 fixation. Electron bifurcation may also occur to provide reduced ferredoxin and reduce ATP expenditure, as demonstrated by Jing et al. (17), although the exact contributions of electron bifurcation and overall energetic efficiency remain unclear.

In the third scenario, the anode potential is −0.15 V and NH_4^+ is absent (Fig. 7C). N_2 fixation occurs at high rates because key N_2 fixation genes (including genes that code for the nitrogenase subunits such as *nifD*) are highly expressed (Fig. 2). At −0.15 V, energy available for biomass production is theoretically limited relative to +0.15 V, resulting in a reduced state for many cytochromes and a shift toward more reduced electron carriers, such as NADH instead of NAD^+ (27). N_2 fixation may be a strategy to reoxidize these carriers by redirecting electrons toward NH_4^+ and H_2 production, thus helping to maintain redox homeostasis under the energy-constrained conditions, as has been observed in other diazotrophs (53, 54). Electron bifurcation through the EtfAB and NfnAB complexes are likely directly involved in reoxidizing NAD(P)H while providing the required electron donors for N_2 fixation. Compared to other pathways that consume energy from the proton motive force (e.g., the Rnf pathway in *A. vinelandii*), this strategy should allow additional ATP to be generated from substrate oxidation and be directly utilized by the nitrogenase to overcome the high energy activation (92). This mechanism has been observed in *A. vinelandii*, where the Fix electron bifurcation system is preferred over Rnf at low O_2 concentrations to maximize energy utilization (93). Although *G. sulfurreducens* does not possess the Fix complex, the EtfAB complex is functionally similar (70), providing support for the idea that this mechanism likely helps energy optimization at −0.15 V and increases N_2 fixation rates. The fixed nitrogen at −0.15 V is stored primarily as glutamine and glutamate to possibly lower the potential toxicity of intracellular NH_4^+, act as a sensing and regulatory molecule as reported in other microorganisms (50), or contribute to redox homeostasis by oxidizing NAD(P)H (52). A regulatory connection between glutamate and glutamine synthesis and electron bifurcation may occur to help N_2 fixation at −0.15 V, because the genes encoding the electron bifurcating system NfnAB, *nfnA* and *nfnB*, are similar to *gltS* (GSU3057 [*nfnA*] has been annotated as a glutamate synthase gene [94]) and the two enzymes have similar amino acid sequences and structures (66, 68). To maximize electron transfer to the anode and obtain energy for N_2 reduction, certain electron-transfer related genes are upregulated, including *omcE* and *pilA* (the latter is dependent on the nitrogen regulon regulator RpoN [28]); however, a better understanding of both proteins is needed to properly characterize their function under N_2 fixation conditions. Posttranslational controls of nitrogenase activity, such as DraG and DraT, are also likely to be involved. Studies on the activities of these nitrogenase-regulating enzymes in *G. sulfurreducens* at different potentials are needed to improve the understanding of regulatory mechanisms involved in the posttranscriptional control of nitrogenase levels and activity.

Conclusions. Our results show that N_2 fixation activity and regulation in *Geobacter sulfurreducens* change with the anode potential in microbial electrolysis cells (MECs). N_2 fixation in free-living diazotrophs such as *G. sulfurreducens* is tightly controlled by several regulatory genes. The use of an MEC to adjust electron acceptor (anode) potentials led to differential gene expression profiles for this organism depending on the applied potential or the addition of fixed nitrogen (i.e., NH_4^+). At an anode potential of −0.15 V versus SHE, N_2 fixation-related genes and flavin-based electron bifurcation genes showed the highest expression relative to +0.15 V, and N_2 fixation rates were found to be elevated. This implies a connection between these processes and a novel route for this organism to optimize electron transfer and N_2 fixation as a means to achieve redox homeostasis under energy-constrained conditions. While we found higher nitrogenase-related gene expression and N_2 fixation rates at −0.15 V, our results are based on the entire anode biofilm, which likely included active and nonactive cells that may have varied in activity and gene expression. To gain finer resolution of gene expression levels throughout the biofilm, extracting RNA during exponential growth and from biofilm sections is needed. Transcriptomics of sectioned biofilms may also help clarify whether expression of N_2 fixation genes changes with proximity to the anode surface. Using an anode as an electron acceptor is a viable approach not only to increase N_2 fixation under anaerobic conditions but also to understand the regulation and connections between N_2 fixation and anode respiration with the intent of optimizing the pathways for NH_4^+ production. Additional experiments, such as studying the effect of NH_4^+ on gene expression profiles at negative anode potentials, elucidating the contribution of posttranslational regulatory mechanisms such as DraG/T, and characterization of the electron bifurcating systems NfnAB and EtfAB in *G. sulfurreducens*, will help reveal metabolic controls of N_2 fixation genes during anode respiration. Targeting NH_4^+ assimilation and transport genes through editing may permit excretion of this compound during anode respiration, while controlling the anode potential to enable increased expression of N_2 fixation genes may provide an operational approach to enhance N_2 fixation rates.

MATERIALS AND METHODS

Reactor assembly and operation. The gas-tight microbial electrolysis cells (MECs) consisted of 100-mL glass medium bottles with rubber stoppers, a polished graphite plate (surface area (A) = 4.5 cm^2) as the anode, and stainless steel mesh (surface area (A) = 3.9 cm^2 projected area) as the cathode. Both electrodes were connected to current collectors (titanium and stainless steel wires, respectively) that were inserted through the rubber stopper. A plastic threaded bolt was used to join the anode and cathode and ensure that the distance between them was fixed at 2 cm. An Ag/AgCl reference electrode (+200 mV versus SHE) was inserted through the rubber stopper and placed between the anode and cathode.

G. sulfurreducens PCA was first grown from a frozen stock in a phosphate-buffered medium (PBM) containing (per liter) 2.5 g NaH_2PO_4, 4.6 g Na_2HPO_4, 0.1 g KCl, 10 mL of a vitamin solution, and 10 mL of a trace mineral solution (95), with sodium acetate (1 g/L) as the electron donor and sodium fumarate (8 g/L) as the electron acceptor and without NH_4^+. After reaching early stationary phase (optical density at 600 nm [OD_{600}] $\approx$ 0.5), 10 mL of suspension was harvested by centrifugation (4,000 rpm for 20 min), and the pellet was resuspended in 100 mL of PBM containing sodium acetate (2 g/L) but no fumarate or NH_4^+. One resuspended pellet was added to each MEC. After addition of medium and inoculum, the MECs were operated in fed-batch mode at 30°C. They were connected to a potentiostat (Bio-Logic Science Instruments, Knoxville, TN) and operated with a fixed E_{AN} of either −0.15 V or +0.15 V versus SHE. To investigate the impact of NH_4^+ on N_2 fixation regulatory pathways, additional reactors were operated at +0.15 V versus SHE with either 0.3 g/L or 0.6 g/L NH_4Cl (~5 mM and 10 mM NH_4^+, respectively) added to the medium. All MECs were flushed with 100% N_2 (ultrahigh purity) at the start of the tests. Current density (I_A) was measured to track metabolic activity of the cultures and calculate electron transfer rates. The media were replaced in a biological safety cabinet (to avoid potential biological contamination) once I_A had been stable for at least three days or, in the case when current dropped after reaching a peak, when I_A had decreased to below 75% of the maximum current at the peak. MECs were operated for three batches to promote sufficient biomass production for RNA extraction. For the third batch, the reactors were operated for two days after refeeding before the anode was harvested to ensure that RNA was obtained when the cells were generating stable current.

RNA extraction and sequencing. Two days after the beginning of the third batch, the anodes were removed and placed directly in RNAprotect bacterial reagent (Qiagen) to preserve total RNA. The anode was vigorously scraped using a sterile razor to remove the biofilm cells, which were deposited in the preserving reagent for 5 min. After the samples were centrifuged (5,000 × *g* for 10 min at 4°C), the supernatant was removed, and the pellets were stored at −80°C until RNA was extracted. RNA extraction was performed using the RNeasy minikit (Qiagen) following the manufacturer's instructions. Lysozyme and proteinase K were used to lyse bacterial cells, and DNase I was added to remove DNA contamination. At least 3 μg of total RNA per sample, all with an A_{260}/A_{280} purity of 2 or higher, was sent to the Genomic Sciences Laboratory (GSL) at North Carolina State University. The RNA samples were subjected to ribodepletion, where rRNA was removed from the samples using the RiboMinus transcriptome isolation kit for bacteria, followed by the RiboMinus concentration module (Thermo Fisher Scientific, Waltham, MA). cDNA libraries for next-generation sequencing were prepared using the NEBNext Ultra RNA library preparation kit for Illumina (New England Biolabs Inc., Ipswich, MA). The average library size was 430 bp with an average insert size of 305 bp. The pooled libraries were sequenced using the Illumina NovaSeq 6000 SP platform, with a read length of 150 paired ends. Around 20 to 25 million sequencing reads per sample were obtained to account for residual rRNA and increase the resolution of the mRNA profiles.

After the sequencing data were obtained, sequencing results were filtered using the Trimmomatic tool to remove adapters and low-quality reads (96). They were subsequently aligned to existing genes using the Bowtie2 software tool, using the genome of *G. sulfurreducens* PCA from the Ensembl Genome platform as a reference (97). Counts of successful alignments and generation of gene tables were performed using the HTSeq software tool (98). Gene tables were analyzed on the R platform, utilizing the DESeq2 package to perform statistical and differential expression analysis (99). Genes of the tested treatments were considered differentially expressed with regard to the reference treatment (+0.15 V, no NH_4^+ added) when $\log_2$ fold expression levels were higher than 2.00 or lower than −2.00 based on previous gene expression studies to minimize the inclusion of biologically nonsignificant genes (36–38), and when the adjusted *P* value was less than 0.05 to minimize FDR.

Nitrogenase assay. We estimated N_2 fixation rates using the acetylene reduction assay (ARA) (100). Since acetylene amendments could impact gene expression, we operated a second set of MECs dedicated to ARA testing. Acetylene was produced via a calcium carbide-H_2O reaction as described previously (101). Residual oxygen was removed from acetylene via excess cystine exposure in sealed serum bottles over 12 h. Oxygen depletion, acetylene content, and ethylene generation were determined by gas chromatography. Gas chromatography was performed using a gas chromatograph equipped with a thermal conductivity detector and a flame ionization detector (model 8610C; SRI Instruments, Torrance, CA). Ethylene concentrations were measured by taking 3-mL samples at 3, 6, and 18 h after injection of acetylene. Total ethylene generated was calculated by combining the concentration measured in the headspace of each reactor with the predicted dissolved concentration based upon Henry's law (coefficient of ethylene, 0.0048 M/atm) (102). To normalize ARA rates, biomass was extracted from the anode by scraping and resuspended in ice-cold phosphate-buffered saline (PBS) buffer (50 mM). Protein content was measured with the Pierce bicinchoninic acid protein assay kit (Thermo Scientific, Waltham, MA) following the manufacturer's protocol.

Metabolite assays. We quantified the concentrations of intracellular and extracellular NH_4^+, glutamate, and glutamine in the MECs. Excretion of glutamate and glutamine into the medium was measured using the Glutamine/Glutamate-Glo assay kit (Promega Corporation). For extracellular measurements, a sample of the suspension was centrifuged at 3,200 × *g* for 5 min to separate cells from the medium. Cells were resuspended in 1 mL of ice-cold 50 mM PBS before measurement using the kit's standard protocol. Intracellular measurements were obtained by scraping the biofilm from each electrode and suspending in 1 mL ice-cold 50 mM PBS. A sample of the full biofilm (100 μL) was taken, and inactivation solution I was added to each of the samples (50 μL), followed by Tris solution I (50 μL). Glutamate and glutamine concentrations were then measured via luminescence (Cytation 5; Biotek) using the kit's standard protocol.

Statistical analyses. Statistical analyses were performed on measurements from triplicate MEC reactors using the Microsoft Excel software. Unpaired *t* tests between treatments were performed to compare maximum current density (I_A), startup time, I_A before RNA harvesting, ethylene production rates, and glutamate and glutamine concentrations, with a *P* value of <0.05 defined as indicating statistical significance.

Data availability. The RNA sequencing data to generate gene expression profiles were deposited in the Sequence Read Archive (SRA) database of the National Center of Biotechnology Information (NCBI) under BioProject accession number PRJNA907487.

SUPPLEMENTAL MATERIAL

Supplemental material is available online only.
SUPPLEMENTAL FILE 1, PDF file, 0.5 MB.
SUPPLEMENTAL FILE 2, XLSX file, 0.1 MB.
SUPPLEMENTAL FILE 3, XLSX file, 0.03 MB.
SUPPLEMENTAL FILE 4, XLSX file, 0.04 MB.

ACKNOWLEDGMENTS

This material is based upon work supported by the National Science Foundation under award number CBET-1840956 and the North Carolina State University Game-Changing Research Incentive Program for Plant Sciences Initiative.

Assistance with ethylene quantification was provided by the North Carolina State University Environmental Engineering Lab Manager, Lisa Castellano.

REFERENCES

1. Erisman JW, Sutton MA, Galloway J, Klimont Z, Winiwarter W. 2008. How a century of ammonia synthesis changed the world. Nat Geosci 1:636–639. https://doi.org/10.1038/ngeo325.
2. Cherkasov N, Ibhadon AO, Fitzpatrick P. 2015. A review of the existing and alternative methods for greener nitrogen fixation. Chem Eng Process Process Intensif 90:24–33. https://doi.org/10.1016/j.cep.2015.02.004.
3. Giddey S, Badwal SPS, Munnings C, Dolan M. 2017. Ammonia as a renewable energy transportation media. ACS Sustain Chem Eng 5:10231–10239. https://doi.org/10.1021/acssuschemeng.7b02219.
4. MacFarlane DR, Cherepanov PV, Choi J, Suryanto BHR, Hodgetts RY, Bakker JM, Ferrero Vallana FM, Simonov AN. 2020. A roadmap to the ammonia economy. Joule 4:1186–1205. https://doi.org/10.1016/j.joule.2020.04.004.
5. Zhou F, Azofra LM, Ali M, Kar M, Simonov AN, McDonnell-Worth C, Sun C, Zhang X, MacFarlane DR. 2017. Electro-synthesis of ammonia from nitrogen at ambient temperature and pressure in ionic liquids. Energy Environ Sci 10:2516–2520. https://doi.org/10.1039/C7EE02716H.
6. Cheng Q. 2008. Perspectives in biological nitrogen fixation research. J Integr Plant Biol 50:786–798. https://doi.org/10.1111/j.1744-7909.2008.00700.x.
7. Aasfar A, Bargaz A, Yaakoubi K, Hilali A, Bennis I, Zeroual Y, Meftah Kadmiri I. 2021. Nitrogen fixing *Azotobacter* species as potential soil biological enhancers for crop nutrition and yield stability. Front Microbiol 12:628379. https://doi.org/10.3389/fmicb.2021.628379.
8. Mus F, Khokhani D, MacIntyre AM, Rugoli E, Dixon R, Ané J-M, Peters JW. 2022. Genetic determinants of ammonium in *nifL* mutants of *Azotobacter vinelandii*. Appl Environ Microbiol 88:e01876-21. https://doi.org/10.1128/aem.01876-21.
9. Sabra W, Zeng A-P, Lünsdorf H, Deckwer W-D. 2000. Effect of oxygen on formation and structure of *Azotobacter vinelandii* alginate and its role in

protecting nitrogenase. Appl Environ Microbiol 66:4037–4044. https://doi.org/10.1128/AEM.66.9.4037-4044.2000.

10. Gallon JR. 1981. The oxygen sensitivity of nitrogenase: a problem for biochemists and micro-organisms. Trends Biochem Sci 6:19–23. https://doi.org/10.1016/0968-0004(81)90008-6.
11. Stams AJM, de Bok FAM, Plugge CM, van Eekert MHA, Dolfing J, Schraa G. 2006. Exocellular electron transfer in anaerobic microbial communities. Environ Microbiol 8:371–382. https://doi.org/10.1111/j.1462-2920.2006.00989.x.
12. Call D, Logan BE. 2008. Hydrogen production in a single chamber microbial electrolysis cell lacking a membrane. Environ Sci Technol 42:3401–3406. https://doi.org/10.1021/es8001822.
13. Ortiz-Medina JF, Grunden AM, Hyman MR, Call DF. 2019. Nitrogen gas fixation and conversion to ammonium using microbial electrolysis cells. ACS Sustain Chem Eng 7:3511–3519. https://doi.org/10.1021/acssuschemeng.8b05763.
14. Lovley DR. 2006. Microbial fuel cells: novel microbial physiologies and engineering approaches. Curr Opin Biotechnol 17:327–332. https://doi.org/10.1016/j.copbio.2006.04.006.
15. Bazylinski DA, Dean AJ, Schüler D, Phillips EJP, Lovley DR. 2000. N_2-dependent growth and nitrogenase activity in the metal-metabolizing bacteria, *Geobacter* and *Magnetospirillum* species. Environ Microbiol 2:266–273. https://doi.org/10.1046/j.1462-2920.2000.00096.x.
16. Yi H, Nevin KP, Kim BC, Franks AE, Klimes A, Tender LM, Lovley DR. 2009. Selection of a variant of *Geobacter sulfurreducens* with enhanced capacity for current production in microbial fuel cells. Biosens Bioelectron 24:3498–3503. https://doi.org/10.1016/j.bios.2009.05.004.
17. Jing X, Liu X, Zhang Z, Wang X, Rensing C, Zhou S. 2022. Anode respiration-dependent biological nitrogen fixation by *Geobacter sulfurreducens*. Water Res 208:117860. https://doi.org/10.1016/j.watres.2021.117860.
18. Coppi MV, Leang C, Sandler SJ, Lovley DR. 2001. Development of a genetic system for *Geobacter sulfurreducens*. Appl Environ Microbiol 67:3180–3187. https://doi.org/10.1128/AEM.67.7.3180-3187.2001.
19. Ueki T, Lovley DR. 2010. Novel regulatory cascades controlling expression of nitrogen-fixation genes in *Geobacter sulfurreducens*. Nucleic Acids Res 38:7485–7499. https://doi.org/10.1093/nar/gkq652.
20. Aelterman P, Freguia S, Keller J, Verstraete W, Rabaey K. 2008. The anode potential regulates bacterial activity in microbial fuel cells. Appl Microbiol Biotechnol 78:409–418. https://doi.org/10.1007/s00253-007-1327-8.
21. Torres CI, Krajmalnik-Brown R, Parameswaran P, Marcus AK, Wanger G, Gorby YA, Rittmann BE. 2009. Selecting anode-respiring bacteria based on anode potential: phylogenetic, electrochemical, and microscopic characterization. Environ Sci Technol 43:9519–9524. https://doi.org/10.1021/es902165y.
22. Zacharoff L, Chan CH, Bond DR. 2016. Reduction of low potential electron acceptors requires the CbcL inner membrane cytochrome of *Geobacter sulfurreducens*. Bioelectrochemistry 107:7–13. https://doi.org/10.1016/j.bioelechem.2015.08.003.
23. Levar CE, Hoffman CL, Dunshee AJ, Toner BM, Bond DR. 2017. Redox potential as a master variable controlling pathways of metal reduction by *Geobacter sulfurreducens*. ISME J 11:741–752. https://doi.org/10.1038/ismej.2016.146.
24. Wei J, Liang P, Cao X, Huang X. 2010. A new insight into potential regulation on growth and power generation of *Geobacter sulfurreducens* in microbial fuel cells based on energy viewpoint. Environ Sci Technol 44:3187–3191. https://doi.org/10.1021/es903758m.
25. Bosch J, Lee K-Y, Hong S-F, Harnisch F, Schröder U, Meckenstock RU. 2014. Metabolic efficiency of *Geobacter sulfurreducens* growing on anodes with different redox potentials. Curr Microbiol 68:763–768. https://doi.org/10.1007/s00284-014-0539-2.
26. Song J, Sasaki D, Sasaki K, Kato S, Kondo A, Hashimoto K, Nakanishi S. 2016. Comprehensive metabolomic analyses of anode-respiring *Geobacter sulfurreducens* cells: the impact of anode-respiration activity on intracellular metabolite levels. Process Biochem 51:34–38. https://doi.org/10.1016/j.procbio.2015.11.012.
27. Korth B, Harnisch F. 2019. Spotlight on the energy harvest of electroactive microorganisms: the impact of the applied anode potential. Front Microbiol 10:1352. https://doi.org/10.3389/fmicb.2019.01352.
28. Leang C, Krushkal J, Ueki T, Puljic M, Sun J, Juárez K, Núñez C, Reguera G, DiDonato R, Postier B, Adkins RM, Lovley DR. 2009. Genome-wide analysis of the RpoN regulon in *Geobacter sulfurreducens*. BMC Genomics 10:331. https://doi.org/10.1186/1471-2164-10-331.
29. Ueki T, Lovley DR. 2010. Genome-wide gene regulation of biosynthesis and energy generation by a novel transcriptional repressor in *Geobacter* species. Nucleic Acids Res 38:810–821. https://doi.org/10.1093/nar/gkp1085.
30. Qiu Y, Nagarajan H, Embree M, Shieu W, Abate E, Juárez K, Cho B-K, Elkins JG, Nevin KP, Barrett CL, Lovley DR, Palsson BO, Zengler K. 2013. Characterizing the interplay between multiple levels of organization within bacterial sigma factor regulatory networks. Nat Commun 4:1755. https://doi.org/10.1038/ncomms2743.
31. Bond DR, Lovley DR. 2003. Electricity production by *Geobacter sulfurreducens* attached to electrodes. Appl Environ Microbiol 69:1548–1555. https://doi.org/10.1128/AEM.69.3.1548-1555.2003.
32. Chadwick GL, Jiménez Otero F, Gralnick JA, Bond DR, Orphan VJ. 2019. NanoSIMS imaging reveals metabolic stratification within current-producing biofilms. Proc Natl Acad Sci U S A 116:20716–20724. https://doi.org/10.1073/pnas.1912498116.
33. Franks AE, Nevin KP, Glaven RH, Lovley DR. 2010. Microtoming coupled to microarray analysis to evaluate the spatial metabolic status of *Geobacter sulfurreducens* biofilms. ISME J 4:509–519. https://doi.org/10.1038/ismej.2009.137.
34. Mahmoud M, Parameswaran P, Torres CI, Rittmann BE. 2017. Electrochemical techniques reveal that total ammonium stress increases electron flow to anode respiration in mixed-species bacterial anode biofilms. Biotechnol Bioeng 114:1151–1159. https://doi.org/10.1002/bit.26246.
35. Belleville P, Strong PJ, Dare PH, Gapes DJ. 2011. Influence of nitrogen limitation on performance of a microbial fuel cell. Water Sci Technol 63:1752–1757. https://doi.org/10.2166/wst.2011.111.
36. Whitham JM, Tirado-Acevedo O, Chinn MS, Pawlak JJ, Grunden AM. 2015. Metabolic response of *Clostridium ljungdahlii* to oxygen exposure. Appl Environ Microbiol 81:8379–8391. https://doi.org/10.1128/AEM.02491-15.
37. Bouzo D, Cokcetin NN, Li L, Ballerin G, Bottomley AL, Lazenby J, Whitchurch CB, Paulsen IT, Hassan KA, Harry EJ. 2020. Characterizing the mechanism of action of an ancient antimicrobial, manuka honey, against *Pseudomonas aeruginosa* using modern transcriptomics. mSystems 5:e00106-20. https://doi.org/10.1128/mSystems.00106-20.
38. McIntosh M, Köchling T, Latz A, Kretz J, Heinen S, Konzer A, Klug G. 2021. A major checkpoint for protein expression in *Rhodobacter sphaeroides* during heat stress response occurs at the level of translation. Environ Microbiol 23:6483–6502. https://doi.org/10.1111/1462-2920.15818.
39. Carbon S, Ireland A, Mungall CJ, Shu S, Marshall B, Lewis S, Web Presence Working Group. 2009. AmiGO: online access to ontology and annotation data. Bioinformatics 25:288–289. https://doi.org/10.1093/bioinformatics/btn615.
40. Kersey PJ, Allen JE, Allot A, Barba M, Boddu S, Bolt BJ, Carvalho-Silva D, Christensen M, Davis P, Grabmueller C, Kumar N, Liu Z, Maurel T, Moore B, McDowall MD, Maheswari U, Naamati G, Newman V, Ong CK, Paulini M, Pedro H, Perry E, Russell M, Sparrow H, Tapanari E, Taylor K, Vullo A, Williams G, Zadissia A, Olson A, Stein J, Wei S, Tello-Ruiz M, Ware D, Luciani A, Potter S, Finn RD, Urban M, Hammond-Kosack KE, Bolser DM, De Silva N, Howe KL, Langridge N, Maslen G, Staines DM, Yates A. 2018. Ensembl Genomes 2018: an integrated omics infrastructure for non-vertebrate species. Nucleic Acids Res 46:D802–D808. https://doi.org/10.1093/nar/gkx1011.
41. Mouser PJ, N'Guessan AL, Elifantz H, Holmes DE, Williams KH, Wilkins MJ, Long PE, Lovley DR. 2009. Influence of heterogeneous ammonium availability on bacterial community structure and the expression of nitrogen fixation and ammonium transporter genes during in situ bioremediation of uranium-contaminated groundwater. Environ Sci Technol 43:4386–4392. https://doi.org/10.1021/es8031055.
42. Holmes DE, O'Neil RA, Chavan MA, N'Guessan LA, Vrionis HA, Perpetua LA, Larrahondo MJ, DiDonato R, Liu A, Lovley DR. 2009. Transcriptome of *Geobacter uraniireducens* growing in uranium-contaminated subsurface sediments. ISME J 3:216–230. https://doi.org/10.1038/ismej.2008.89.
43. Oetjen J, Reinhold-Hurek B. 2009. Characterization of the DraT/DraG system for posttranslational regulation of nitrogenase in the endophytic betaproteobacterium *Azoarcus* sp. strain BH72. J Bacteriol 191:3726–3735. https://doi.org/10.1128/JB.01720-08.
44. Zhang Y, Burris RH, Roberts GP. 1992. Cloning, sequencing, mutagenesis, and functional characterization of *draT* and *draG* genes from *Azospirillum brasilense*. J Bacteriol 174:3364–3369. https://doi.org/10.1128/jb.174.10.3364-3369.1992.
45. Heiniger EK, Oda Y, Samanta SK, Harwood CS. 2012. How posttranslational modification of nitrogenase is circumvented in *Rhodopseudomonas palustris* strains that produce hydrogen gas constitutively. Appl Environ Microbiol 78:1023–1032. https://doi.org/10.1128/AEM.07254-11.

46. Schulz AA, Collett HJ, Reid SJ. 2001. Nitrogen and carbon regulation of glutamine synthetase and glutamate synthase in *Corynebacterium glutamicum* ATCC 13032. FEMS Microbiol Lett 205:361–367. https://doi.org/10.1111/j.1574-6968.2001.tb10973.x.
47. Hagen WR, Vanoni MA, Rosenbaum K, Schnackerz KD. 2000. On the iron-sulfur clusters in the complex redox enzyme dihydropyrimidine dehydrogenase. Eur J Biochem 267:3640–3646. https://doi.org/10.1046/j.1432-1327.2000.01393.x.
48. Krushkal J, Juárez K, Barbe JF, Qu Y, Andrade A, Puljic M, Adkins RM, Lovley DR, Ueki T. 2010. Genome-wide survey for PilR recognition sites of the metal-reducing prokaryote *Geobacter sulfurreducens*. Gene 469:31–44. https://doi.org/10.1016/j.gene.2010.08.005.
49. Makemson JC, Hastings JW. 1979. Glutamate functions in osmoregulation in a marine bacterium. Appl Environ Microbiol 38:178–180. https://doi.org/10.1128/aem.38.1.178-180.1979.
50. Feehily C, Karatzas KAG. 2013. Role of glutamate metabolism in bacterial responses towards acid and other stresses. J Appl Microbiol 114:11–24. https://doi.org/10.1111/j.1365-2672.2012.05434.x.
51. Goude R, Renaud S, Bonnassie S, Bernard T, Blanco C. 2004. Glutamine, glutamate, and α-glucosylglycerate are the major osmotic solutes accumulated by *Erwinia chrysanthemi* strain 3937. Appl Environ Microbiol 70:6535–6541. https://doi.org/10.1128/AEM.70.11.6535-6541.2004.
52. McCully AL, Onyeziri MC, LaSarre B, Gliessman JR, McKinlay JB. 2020. Reductive tricarboxylic acid cycle enzymes and reductive amino acid synthesis pathways contribute to electron balance in a *Rhodospirillum rubrum* Calvin-cycle mutant. Microbiology (Reading) 166:199–211. https://doi.org/10.1099/mic.0.000877.
53. Wang D, Zhang Y, Welch E, Li J, Roberts GP. 2010. Elimination of Rubisco alters the regulation of nitrogenase activity and increases hydrogen production in *Rhodospirillum rubrum*. Int J Hydrogen Energy 35:7377–7385. https://doi.org/10.1016/j.ijhydene.2010.04.183.
54. Luxem KE, Kraepiel AML, Zhang L, Waldbauer JR, Zhang X. 2020. Carbon substrate re-orders relative growth of a bacterium using Mo-, V-, or Fe-nitrogenase for nitrogen fixation. Environ Microbiol 22:1397–1408. https://doi.org/10.1111/1462-2920.14955.
55. Scarabotti F, Rago L, Bühler K, Harnisch F. 2021. The electrode potential determines the yield coefficients of early-stage *Geobacter sulfurreducens* biofilm anodes. Bioelectrochemistry 140:107752. https://doi.org/10.1016/j.bioelechem.2021.107752.
56. Klugkist J, Haaker H. 1984. Inhibition of nitrogenase activity by ammonium chloride in *Azotobacter vinelandii*. J Bacteriol 157:148–151. https://doi.org/10.1128/jb.157.1.148-151.1984.
57. Dixon R, Kahn D. 2004. Genetic regulation of biological nitrogen fixation. Nat Rev Microbiol 2:621–631. https://doi.org/10.1038/nrmicro954.
58. Methé BA, Nelson KE, Eisen JA, Paulsen IT, Nelson W, Heidelberg JF, Wu D, Wu M, Ward N, Beanan MJ, Dodson RJ, Madupu R, Brinkac LM, Daugherty SC, DeBoy RT, Durkin AS, Gwinn M, Kolonay JF, Sullivan SA, Haft DH, Selengut J, Davidsen TM, Zafar N, White O, Tran B, Romero C, Forberger HA, Weidman J, Khouri H, Feldblyum TV, Utterback TR, Van Aken SE, Lovley DR, Fraser CM. 2003. Genome of *Geobacter sulfurreducens*: metal reduction in subsurface environments. Science 302:1967–1969. https://doi.org/10.1126/science.1088727.
59. Jung H, Pirch T, Hilger D. 2006. Secondary transport of amino acids in prokaryotes. J Membr Biol 213:119–133. https://doi.org/10.1007/s00232-006-0880-x.
60. Bičáková O, Straka P. 2012. Production of hydrogen from renewable resources and its effectiveness. Int J Hydrogen Energy 37:11563–11578. https://doi.org/10.1016/j.ijhydene.2012.05.047.
61. Coppi MV, O'Neil RA, Lovley DR. 2004. Identification of an uptake hydrogenase required for hydrogen-dependent reduction of Fe(III) and other electron acceptors by *Geobacter sulfurreducens*. J Bacteriol 186:3022–3028. https://doi.org/10.1128/JB.186.10.3022-3028.2004.
62. Coppi MV. 2005. The hydrogenases of *Geobacter sulfurreducens*: a comparative genomic perspective. Microbiology (Reading) 151:1239–1254. https://doi.org/10.1099/mic.0.27535-0.
63. Thauer RK, Kaster A-K, Seedorf H, Buckel W, Hedderich R. 2008. Methanogenic archaea: ecologically relevant differences in energy conservation. Nat Rev Microbiol 6:579–591. https://doi.org/10.1038/nrmicro1931.
64. Croese E, Jeremiasse AW, Marshall IPG, Spormann AM, Euverink G-JW, Geelhoed JS, Stams AJM, Plugge CM. 2014. Influence of setup and carbon source on the bacterial community of biocathodes in microbial electrolysis cells. Enzyme Microb Technol 61-62:67–75. https://doi.org/10.1016/j.enzmictec.2014.04.019.
65. Tremblay P-L, Lovley DR. 2012. Role of the NiFe hydrogenase Hya in oxidative stress defense in *Geobacter sulfurreducens*. J Bacteriol 194:2248–2253. https://doi.org/10.1128/JB.00044-12.
66. Peters JW, Miller A-F, Jones AK, King PW, Adams MW. 2016. Electron bifurcation. Curr Opin Chem Biol 31:146–152. https://doi.org/10.1016/j.cbpa.2016.03.007.
67. Buckel W, Thauer RK. 2018. Flavin-based electron bifurcation, a new mechanism of biological energy coupling. Chem Rev 118:3862–3886. https://doi.org/10.1021/acs.chemrev.7b00707.
68. Liang J, Huang H, Wang S. 2019. Distribution, evolution, catalytic mechanism, and physiological functions of the flavin-based electron-bifurcating NADH-dependent reduced ferredoxin:NADP$^+$ oxidoreductase. Front Microbiol 10:373. https://doi.org/10.3389/fmicb.2019.00373.
69. Garcia Costas AM, Poudel S, Miller A-F, Schut GJ, Ledbetter RN, Fixen KR, Seefeldt LC, Adams MWW, Harwood CS, Boyd ES, Peters JW. 2017. Defining electron bifurcation in the electron-transferring flavoprotein family. J Bacteriol 199:e00440-17. https://doi.org/10.1128/JB.00440-17.
70. Ledbetter RN, Garcia Costas AM, Lubner CE, Mulder DW, Tokmina-Lukaszewska M, Artz JH, Patterson A, Magnuson TS, Jay ZJ, Duan HD, Miller J, Plunkett MH, Hoben JP, Barney BM, Carlson RP, Miller A-F, Bothner B, King PW, Peters JW, Seefeldt LC. 2017. The electron bifurcating FixABCX protein complex from *Azotobacter vinelandii*: generation of low-potential reducing equivalents for nitrogenase catalysis. Biochemistry 56:4177–4190. https://doi.org/10.1021/acs.biochem.7b00389.
71. Geelhoed JS, Henstra AM, Stams AJM. 2016. Carboxydotrophic growth of *Geobacter sulfurreducens*. Appl Microbiol Biotechnol 100:997–1007. https://doi.org/10.1007/s00253-015-7033-z.
72. Chan CH, Levar CE, Jiménez-Otero F, Bond DR. 2017. Genome scale mutational analysis of *Geobacter sulfurreducens* reveals distinct molecular mechanisms for respiration and sensing of poised electrodes versus Fe(III) oxides. J Bacteriol 199:e00340-17. https://doi.org/10.1128/JB.00340-17.
73. Stephen CS, LaBelle EV, Brantley SL, Bond DR. 2014. Abundance of the multiheme c-type cytochrome OmcB increases in outer biofilm layers of electrode-grown *Geobacter sulfurreducens*. PLoS One 9:e104336. https://doi.org/10.1371/journal.pone.0104336.
74. Methe BA, Webster J, Nevin K, Butler J, Lovley DR. 2005. DNA microarray analysis of nitrogen fixation and Fe(III) reduction in *Geobacter sulfurreducens*. Appl Environ Microbiol 71:2530–2538. https://doi.org/10.1128/AEM.71.5.2530-2538.2005.
75. Nevin KP, Kim B-C, Glaven RH, Johnson JP, Woodard TL, Methé BA, DiDonato RJ, Covalla SF, Franks AE, Liu A, Lovley DR. 2009. Anode biofilm transcriptomics reveals outer surface components essential for high density current production in *Geobacter sulfurreducens* fuel cells. PLoS One 4:e5628. https://doi.org/10.1371/journal.pone.0005628.
76. Mehta T, Coppi MV, Childers SE, Lovley DR. 2005. Outer membrane c-type cytochromes required for Fe(III) and Mn(IV) oxide reduction in *Geobacter sulfurreducens*. Appl Environ Microbiol 71:8634–8641. https://doi.org/10.1128/AEM.71.12.8634-8641.2005.
77. Shi L, Richardson DJ, Wang Z, Kerisit SN, Rosso KM, Zachara JM, Fredrickson JK. 2009. The roles of outer membrane cytochromes of *Shewanella* and *Geobacter* in extracellular electron transfer. Environ Microbiol Rep 1:220–227. https://doi.org/10.1111/j.1758-2229.2009.00035.x.
78. Holmes DE, Chaudhuri SK, Nevin KP, Mehta T, Methé BA, Liu A, Ward JE, Woodard TL, Webster J, Lovley DR. 2006. Microarray and genetic analysis of electron transfer to electrodes in *Geobacter sulfurreducens*. Environ Microbiol 8:1805–1815. https://doi.org/10.1111/j.1462-2920.2006.01065.x.
79. Wang F, Mustafa K, Suciu V, Joshi K, Chan CH, Choi S, Su Z, Si D, Hochbaum AI, Egelman EH, Bond DR. 2022. Cryo-EM structure of an extracellular *Geobacter* OmcE cytochrome filament reveals tetrahaem packing. Nat Microbiol 7:1291–1300. https://doi.org/10.1038/s41564-022-01159-z.
80. Santos TC, Silva MA, Morgado L, Dantas JM, Salgueiro CA. 2015. Diving into the redox properties of *Geobacter sulfurreducens* cytochromes: a model for extracellular electron transfer. Dalton Trans 44:9335–9344. https://doi.org/10.1039/c5dt00556f.
81. Ishii S, Suzuki S, Tenney A, Nealson KH, Bretschger O. 2018. Comparative metatranscriptomics reveals extracellular electron transfer pathways conferring microbial adaptivity to surface redox potential changes. ISME J 12:2844–2863. https://doi.org/10.1038/s41396-018-0238-2.
82. Hernández-Eligio A, Pat-Espadas AM, Vega-Alvarado L, Huerta-Amparán M, Cervantes FJ, Juárez K. 2020. Global transcriptional analysis of *Geobacter sulfurreducens* under palladium reducing conditions reveals new key cytochromes involved. Appl Microbiol Biotechnol 104:4059–4069. https://doi.org/10.1007/s00253-020-10502-5.

83. Deng X, Dohmae N, Nealson KH, Hashimoto K, Okamoto A. 2018. Multiheme cytochromes provide a pathway for survival in energy-limited environments. Sci Adv 4:eaao5682. https://doi.org/10.1126/sciadv.aao5682.
84. Richter LV, Sandler SJ, Weis RM. 2012. Two isoforms of *Geobacter sulfurreducens* PilA have distinct roles in pilus biogenesis, cytochrome localization, extracellular electron transfer, and biofilm formation. J Bacteriol 194:2551–2563. https://doi.org/10.1128/JB.06366-11.
85. Saikia SP, Jain V. 2007. Biological nitrogen fixation with non-legumes: an achievable target or a dogma? Curr Sci 92:317–322. https://doi.org/10.2307/24096726.
86. Reitzer L. 2003. Nitrogen assimilation and global regulation in *Escherichia coli*. Annu Rev Microbiol 57:155–176. https://doi.org/10.1146/annurev.micro.57.030502.090820.
87. Cheng S, Logan BE. 2008. Evaluation of catalysts and membranes for high yield biohydrogen production via electrohydrogenesis in microbial electrolysis cells (MECs). Water Sci Technol 58:853–857. https://doi.org/10.2166/wst.2008.617.
88. Marozava S, Röling WFM, Seifert J, Küffner R, von Bergen M, Meckenstock RU. 2014. Physiology of *Geobacter metallireducens* under excess and limitation of electron donors. Part II. Mimicking environmental conditions during cultivation in retentostats. Syst Appl Microbiol 37:287–295. https://doi.org/10.1016/j.syapm.2014.02.005.
89. Greening C, Cook GM. 2014. Integration of hydrogenase expression and hydrogen sensing in bacterial cell physiology. Curr Opin Microbiol 18:30–38. https://doi.org/10.1016/j.mib.2014.02.001.
90. Poudel S, Colman DR, Fixen KR, Ledbetter RN, Zheng Y, Pence N, Seefeldt LC, Peters JW, Harwood CS, Boyd ES. 2018. Electron transfer to nitrogenase in different genomic and metabolic backgrounds. J Bacteriol 200:e00757-17. https://doi.org/10.1128/JB.00757-17.
91. Alleman AB, Mus F, Peters JW. 2021. Metabolic model of the nitrogen-fixing obligate aerobe *Azotobacter vinelandii* predicts its adaptation to oxygen concentration and metal availability. mBio 12:e02593-21. https://doi.org/10.1128/mBio.02593-21.
92. Buckel W, Thauer RK. 2018. Flavin-based electron bifurcation, ferredoxin, flavodoxin, and anaerobic respiration with protons (Ech) or NAD^+ (Rnf) as electron acceptors: a historical review. Front Microbiol 9:401. https://doi.org/10.3389/fmicb.2018.00401.
93. Alleman AB, Garcia CA, Mus F, Peters JW. 2022. Rnf and Fix have specific roles during aerobic nitrogen fixation in *Azotobacter vinelandii*. Appl Environ Microbiol 88:e01049-22. https://doi.org/10.1128/aem.01049-22.
94. Coppi MV, O'Neil RA, Leang C, Kaufmann F, Methé BA, Nevin KP, Woodard TL, Liu A, Lovley DR. 2007. Involvement of *Geobacter sulfurreducens* SfrAB in acetate metabolism rather than intracellular, respiration-linked Fe(III) citrate reduction. Microbiology (Reading) 153:3572–3585. https://doi.org/10.1099/mic.0.2007/006478-0.
95. Call DF, Logan BE. 2011. A method for high throughput bioelectrochemical research based on small scale microbial electrolysis cells. Biosens Bioelectron 26:4526–4531. https://doi.org/10.1016/j.bios.2011.05.014.
96. Bolger AM, Lohse M, Usadel B. 2014. Trimmomatic: a flexible trimmer for Illumina sequence data. Bioinformatics 30:2114–2120. https://doi.org/10.1093/bioinformatics/btu170.
97. Langmead B, Salzberg SL. 2012. Fast gapped-read alignment with Bowtie 2. Nat Methods 9:357–359. https://doi.org/10.1038/nmeth.1923.
98. Anders S, Pyl PT, Huber W. 2015. HTSeq–a Python framework to work with high-throughput sequencing data. Bioinformatics 31:166–169. https://doi.org/10.1093/bioinformatics/btu638.
99. Love MI, Huber W, Anders S. 2014. Moderated estimation of fold change and dispersion for RNA-seq data with DESeq2. Genome Biol 15:550. https://doi.org/10.1186/s13059-014-0550-8.
100. Hardy RWF, Holsten RD, Jackson EK, Burns RC. 1968. The acetylene-ethylene assay for N_2 fixation: laboratory and field evaluation. Plant Physiol 43:1185–1207. https://doi.org/10.1104/pp.43.8.1185.
101. Hyman MR, Arp DJ. 1987. Quantification and removal of some contaminating gases from acetylene used to study gas-utilizing enzymes and microorganisms. Appl Environ Microbiol 53:298–303. https://doi.org/10.1128/aem.53.2.298-303.1987.
102. Sander R. 2015. Compilation of Henry's law constants (version 4.0) for water as solvent. Atmos Chem Phys 15:4399–4981. https://doi.org/10.5194/acp-15-4399-2015.